CrystEngComm

Accepted Manuscript

ROYAL SOCIETY OF CHEMISTRY

www.rsc.org/crystengcomm

New 4-(2-(4-alkoxyphenyl)-6-methoxypyridin-4-yl)benzonitriles: Synthesis, liquid crystalline behavior and photophyscial properties

Ahipa. T. N.,[a] Vijith Kumar,[b] D. S. Shankar Rao,[c] Subbarao Krishna Prasad,[c] and Airody Vasudeva Adhikari [a]*

[a] Department of Chemistry, National Institute of Technology Karnataka, Surathkal, Mangalore - 575 025, India.

[b] Solid State Structural Chemistry Unit, Indian Institute of Science, Bangalore - 560 012, India.

[c] Centre for Soft Matter Research, Jalahalli, Bangalore - 560 013, India.

* Corresponding author. Tel.: +91 8242474046; fax: +918242474033.

E-mail addresses: avachem@gmail.com, avadhikari123@yahoo.co.in, avchem@nitk.ac.in.

ABSTRACT

A new series of luminescent 4-(2-(4-alkoxyphenyl)-6-methoxypyridin-4-yl)benzonitriles carrying three ring system, *viz*. methoxy pyridine, benzonitrile and alkxoy benzene with variable allkoxy chain length, holding bent-core structure was synthesized as potential mesogens and characterized by spectral techniques. Their liquid crystalline behavior was investigated by polarizing optical microscopy (POM), differential scanning calorimetry (DSC) and variable temperature powder X-ray diffraction (PXRD) measurements. The study reveals that compound with shorter chain length [*i.e.* m=4] exhibits exclusively nematic phase while compounds with higher chain lengths [*i.e.* m=6-14 (only even)] show predominantly orthorhombic columnar phase. The single crystal X-ray analysis of 4-(2-(4-butyloxy/octyloxyphenyl)-6-methoxypyridin-

4-yl)benzonitriles reveals that they possess slightly non-planar unsymmetrical bent structure and their molecular packing consists of nonconventional H-bond interactions; further it explains the observed liquid crystalline phase. The optical study indicates that title compounds are good blue emitting materials showing absorption and emission bands in the range of 335-345 nm and 415-460 nm, respectively. The electrochemical study of 4-(2-(4-octyloxyphenyl)-6-methoxypyridin-4-yl)benzonitrile shows a band gap 1.89 eV with HOMO and LUMO energy levels of -5.06 and -3.17 eV, respectively. Also, density functional theory (DFT) calculations confirm its optimized geometry, electronic absorption and frontier molecular orbital distributions.

KEYWORDS: Methoxypyridine; Crystal structure; Hydrogen bond; Liquid crystal; Optical property.

INTRODUCTION

Luminescent liquid crystals (LLCs) have received significant attention because of their favorable molecular self-assembly with intrinsic light generation capabilities. Because of these unique properties they are quite useful in novel optical device applications such as emissive LC displays,[1-4] polarized dye lasers,[5-7] anisotropic organic light-emitting diodes (OLEDs),[8-10] and ordered electron transport systems.[8,11] In this context, several molecular architectures involving rod-, bent-, or disc shaped arrangements have been designed and reported in the literature as active LLCs for device applications.[12-15] Owing to their importance in optoelectronic field, the quest for the development of new materials with both liquid crystal (LC) and emissive behavior has gained much momentum. It is well-established that proper structural modifications on luminescent systems with suitably positioned variable alkoxy chains and highly electron withdrawing cyano group as substituents leads to display complex mesogenic as well as photo-

emissive properties. Here, the polar cyano functionality acts as highly polarisable group, and ability to enhance the overall polarisable anisotropy, which results in high clearing points.[16] In addition, introduction of asymmetry and shape anisotropic factors in such systems offers a significant contribution in achieving LC properties.[17]

Amongst the various luminescent materials reported in the literature, compounds carrying heterocyclic systems such as pyridine,[18] pyrazole,[19] oxadiazole,[20] and triazole,[21] were found to be interesting mesogens with high charge carrier mobility. Evidently, their mesogenic property is attributed to the enhanced unsaturation and polarizability caused by insertion of heteroaromatics. Also, pyridine and oxadiazole based mesogens were reported to possess bent shaped structure. Moreover, pyridine based mesogens were shown to be thermally and photochemically stable photoactive materials with high quantum efficiency as well as good charge transporting ability. In this approach, our research group successfully designed and synthesized new bent-shaped donor-acceptor type 2-methoxy-3-cyanopyridines carrying three ring systems, as intrinsic LLC materials.[22] These compounds exhibit ambient temperature rectangular columnar phase with blue emissive behavior in both solution as well as in LC states.

Against this background, we have designed six new pyridine derivatives (**4a-f**) with pyridine as a central core, by incorporating electron donating methoxy group as a lateral substituent at position-6, electron releasing 4-alkoxyphenyl moiety at its position-2, and electron withdrawing 4-cyanophenyl ring at position-4 of pyridine, in order to achieve an unsymmetrical bent shaped molecular architecture. Since, some of the substituted pyridines were shown to be good luminescent mesogens and electron transporting materials,[23] the newly designed molecules are expected to exhibit good luminescent liquid crystalline behavior. Accordingly, we have

synthesized six new 4-(2-(4-alkoxyphenyl)-6-methoxypyridin-4-yl)benzonitriles (**4a-f**) from 4-(3-(4-alkoxyphenyl)-3-oxoprop-1-enyl)benzonitrile (**3a-f**) via base catalyzed cyclization using malononitrile (**2**). They were well characterized with the aid of FTIR, ^{1}H NMR, ^{13}C NMR, mass spectral, elemental analyses and single crystal X-ray diffraction (SCXRD) study. Their phase transitions and mesogenic properties were identified by using POM, DSC and PXRD techniques. Also, the influence of variation in terminal alkoxy chain lengths [i.e. m=4-14 (only even)] on their mesogenic property was studied.

Further, they were subjected to UV-visible absorption and photo-luminescent studies in order to investigate their optical behavior. Furthermore, SCXRD study was performed on compounds **4a** and **4c**, in order to obtain full information on their 3-D molecular structure including packing fraction, molecular orientation, molecular interactions and to support the observed mesophase behavior. The electrochemical analysis was carried out on one of the representative compounds **4c** in order to determine its electrochemical band gap as well as its HOMO and LUMO energy levels. Finally, quantum chemistry density functional theory (DFT) calculations at def2 TZVP basis set were performed to acquire knowledge on optimized geometry, electronic absorption, and frontier molecular orbitals.

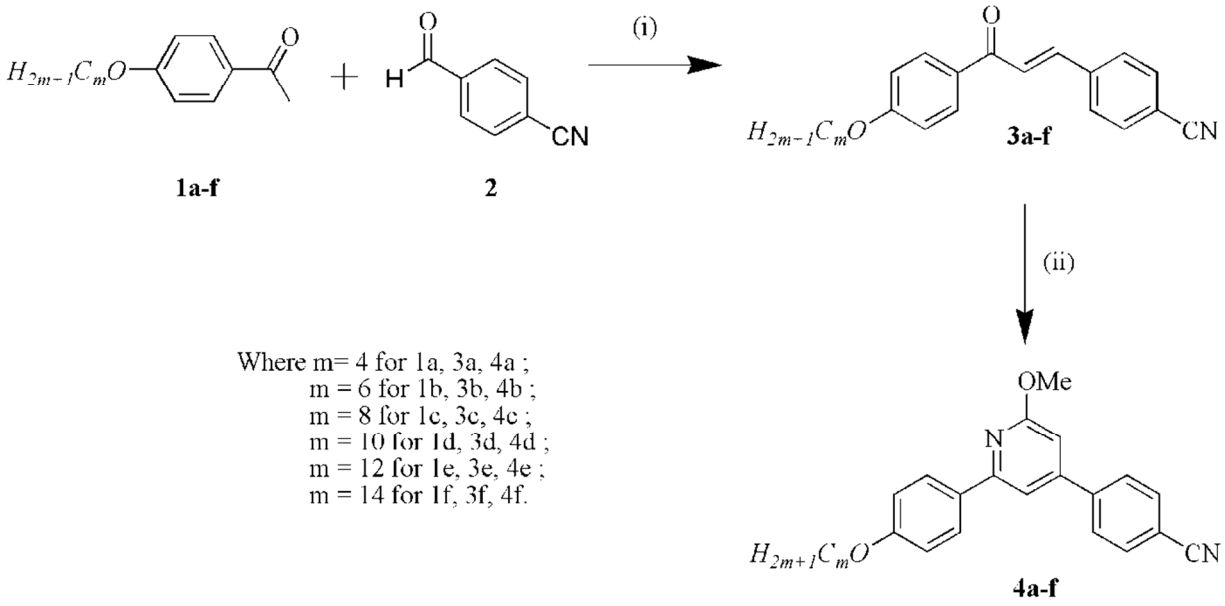

Scheme 1. Synthesis of new methoxypyridines. Reagents and conditions: (i) KOH / EtOH, rt; (ii) Malononitrile, NaOMe, MeOH, rt.

RESULTS AND DISCUSSION

SYNTHESIS AND STRUCTURE CHARACTERIZATION

The synthetic route for the preparation of the target compounds is shown in Scheme 1. The starting materials (**1a-f**) were prepared in good yield by reacting various alkyl bromides [m=4-14 (only even)] with 4-hydroxyacetophenone according to the reported procedure.[24] The required chalcone (**3a-f**) was prepared from (**1a-f**) and 4-cyanobenzaldehyde **2** using Claisen - Schmidth reaction and finally they were cyclized to obtain methoxypyridine derivatives (**4a-f**) by condensing them with malononitrile in presence of sodium methoxide at room temperature. Interestingly, methoxypyridine derivatives (**4a-f**) were obtained as cyclized products instead of predicted 4-(4-cyanophenyl)-2-methoxy-6-(4-(alkoxy)phenyl)nicotinonitrile**s**. Here, presence of electron withdrawing cyano group attached to phenyl ring facilitated condensation followed by

dehydrocyanation, rather than condensation with dehydrogenation.[25-27] Further, crystal structure analysis of **4a** and **4c** evidences the observed fact.

Newly synthesized compounds including intermediates were characterized and identified by FTIR, ^{1}H NMR, ^{13}C NMR and Mass spectroscopy. Further, their analytical purity was determined by elemental analysis. The compound **4a**, in its FTIR spectrum showed two strong absorption bands at 2944 and 2859 cm^{-1} that correspond to asymmetric and symmetrical C-H stretching vibrations of methylene. Further, the appearance of strong band at 2219 cm^{-1} indicated the presence of cyano group in its molecular structure. Also, appearance of one more strong peak at 1577 cm^{-1} that accounts for C=N stretching vibrations, confirmed the formation of central methoxypyridine via cyclization reaction. Further, its ^{1}H NMR spectrum showed unique resonance at δ 8.05, 7.84, 7.77 and 7.01 ppm for the protons of aromatic moieties. Appearance of two singlets at δ 7.46 and 6.82 ppm for the presence of single protons at positions-3 and -5 of pyridine ring confirmed its structure. In addition, three protons of methoxy substituent at position-6 of pyridine ring resonated at δ 4.22 ppm as singlet, which further confirmed the construction of central pyridine ring. Furthermore, the appearance of primary and secondary proton signals in the range of δ 1.86-1.00 ppm in its ^{1}H NMR spectrum confirmed the presence of terminal butoxy chain in compound **4a**. In its ^{13}C NMR spectrum, twelve distinct signals were observed at downfield due to one pyridine ring and two aromatic ring carbon atoms. The carbon carrying methoxy group and cyano group, and carbon of cyano group attached to aromatic resonate at 164.47, 115.19 and 112.05 ppm, respectively, confirming the formation of methoxypyridine ring. The two kinds of quaternary carbon atom of pyridine ring resonate at 155.57 and 149.90 ppm, respectively. In addition, two kind of tertiary carbon atom resonates at 110.57 and 106.31 ppm, respectively. The quaternary carbon atoms connected to oxygen

resonate in the region of 164.47-160.31 ppm. The primary and secondary carbon peaks of aliphatic chains appeared in the region of 68.25-14.08 ppm. Finally, its mass spectrum showed the $[M+H]^+$ peak at 359.1, which matches with the calculated molecular weight for the formula of $C_{23}H_{23}N_2O_2$.

MESOMORPHIC BEHAVIOR

The transition temperatures and phase assignments of **4a-f** were investigated by POM and DSC. Results of their phase transition temperatures with enthalpies are summarized in Table 1. Compound **4a** displays characteristic nematic phase sequence under POM observation (Figure 1(a)). On slow cooling from isotropic to LC phase; it exhibits a marble texture, which is characteristic of nematic phase. Its enantiotropic phase transitions were observed in its DSC trace (Figure S1; ESI†) under heating and cooling cycle. Further, compound **4a** melts to the nematic phase at about 127 °C and isotropizes at about 142 °C at a heating rate of 10 °C per minute. On cooling, it retains the nematic phase till 98 °C, below which its crystallization begins. The observed DSC phase transition temperatures are in agreement with the POM observations of it. Also, PXRD measurements were carried out for the compound at its nematic phase. The obtained diffraction pattern of **4a** is shown in Figure S2 (ESI†). In its PXRD pattern, the diffuse wide angle scattering observed at 3.6 Å corresponds to the mean lateral distance between the molecules and it evidences the existence of fluidic nature in the nematic phase. In addition, the diffuse small angle scattering was observed at 16.6 Å, which is quite a bit smaller than the calculated molecular length (19.07 Å). Here, the observed small angle scattering pattern is in agreement with the diffraction profile obtained for the nematogens reported in the literature.[28]

Further, its intensity is found to be lower than that of wide angle scattering, mainly due to the presence of shorter butoxy chain in compound **4a**.

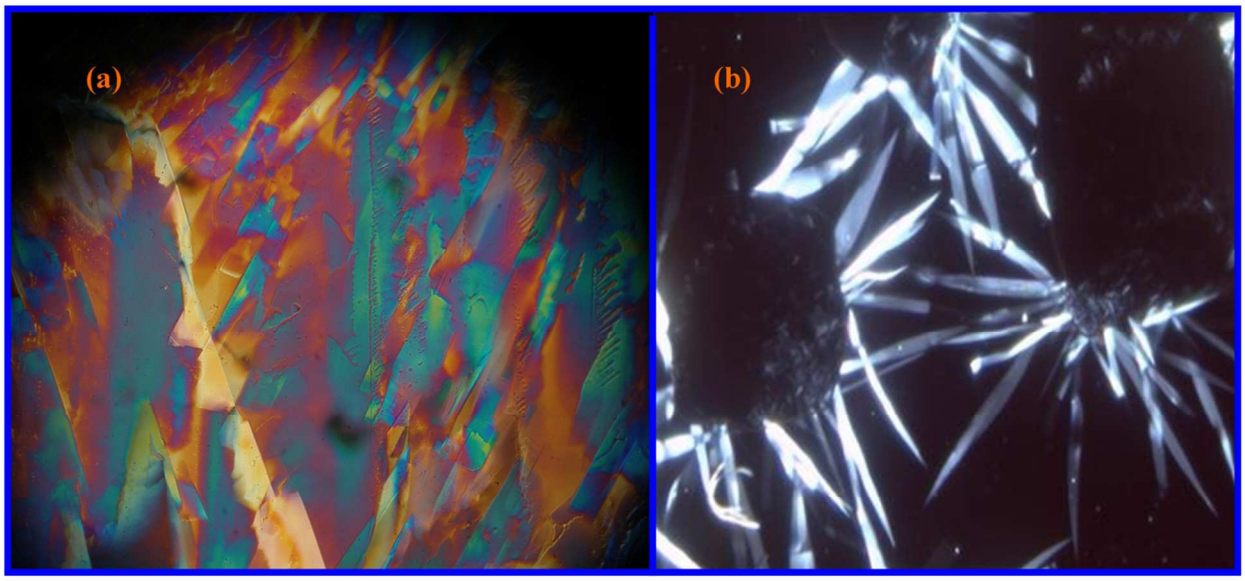

Figure 1. Photomicrographs of (a) marble texture in the nematic phase of **4a** at 137 °C; (b) plastic orthorhombic columnar phase of **4e** at 102 °C.

Table 1. Phase transitions and enthalpies of **4a-f**

Compound	m	Transition	Temperature/ ^{0}C	ΔH/kJ mol^{-1}
4a	4	Cr-N	127.1	10.6
		N-I	142.8	0.8
4b	6	Cr-Col_{ortho}	105.5	14.8
		Col_{ortho}-I	125.2	2.3
4c	8	Cr-Col_{ortho}	105.1	5.9
		Col_{ortho}-I	121.4	1.4
4d	10	Cr-Col_{ortho}	102.6	21.2

		Col_{ortho}-I	120.5	4.3
4e	12	Cr-Col_{ortho}	101.6	13.2
		Col_{ortho}-I	118.2	1.4
4f	14	Cr-Col_{ortho}	99.3	26.1
		Col_{ortho}-I	113.3	3.7

Note: Cr: crystal; N: nematic; Col_{ortho}: orthorhombic columnar; I: isotropic liquid

Compounds **4b-f** [m= 6-14 (only even)] with longer alkoxy terminal groups on cooling from isotropic phase, exhibit a more ordered phase with birefrigent textures under POM observation. Further, characterization using X-ray diffraction measurement on compound **4e** confirms the columnar nature of the underlying structure of these intermediate phases; the results of which are summarized in Table S1 (ESI†). Raw X-ray profiles obtained in the mesophase for a representative compound, **4e**, is shown in Figure 2. X-ray diffraction pattern of **4e** at 104 °C, exhibits a number of sharp peaks (in both small and wide angle regions). The obtained pattern was subjected to peak fitting and indexing analysis which confirms that the observed mesophase has a columnar structure characterized by an orthorhombic symmetry with lattice parameters a= 43.44Å, b= 14.47Å, c= 4.49Å, $\alpha = \beta = \gamma = 90°$ (as shown in Figure 2 obtained after background subtraction). Additionally, a diffused halo peak at ~ 4.3 Å was still observed in the wider angle regions, ruling out the phase to be a truly crystalline one. Thus, we have proposed the phase to be a plastic columnar phase, i.e. a phase which has positional ordering in all the three dimensions, while still retaining certain orientational degrees of freedom.[29,30] The fact that the spacing of the first reflection is lower than the length of the molecule obtained from molecular modeling (29.2 Å), and being indexed to (200) suggested that the in-plane rectangular lattice consists of two

molecules, perhaps held together by the non-conventional intermolecular hydrogen-bonding. Figure 1(b) represents the plastic orthorhombic columnar phase observed under POM for **4e**, while Figure 3 shows the DSC trace of **4f**.

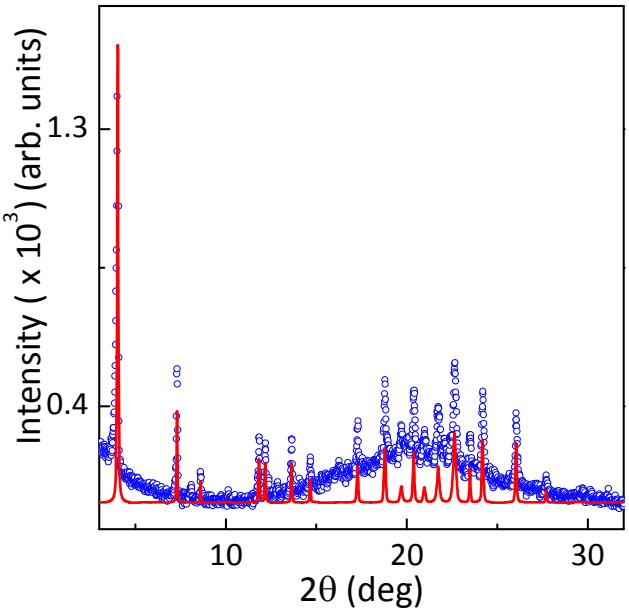

Figure 2. Powder X-ray diffraction pattern of **4e** at 104 °C. The blue circles indicate measured data and the red line shows the profile fitting after background correction.

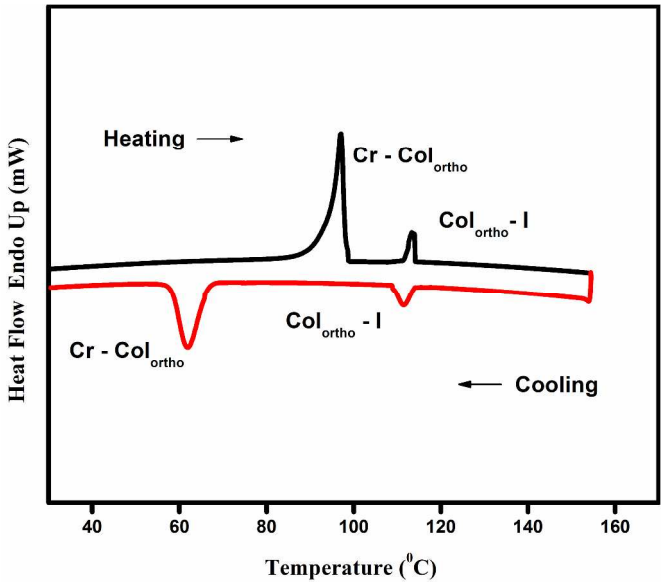

Figure 3. DSC trace of **4f**.

Table 2. Crystal data and structure refinement for compounds **4a** and **4c**

Compound	**4a**	**4c**
Formula	$C_{23}H_{22}N_2O_2$	$C_{27}H_{30}N_2O_2$
Formula weight	358.43	414.53
CCDC number	958625	909202
Temperature (K)	296(2)	120(2)
Crystal form	Block	Block
Color	Colorless	Colorless
Crystal system	Triclinic	Triclinic
Space group	*P-1*	*P-1*
a (Å)	8.978(3)	8.148(3)
b (Å)	10.677(3)	10.726(3)
c (Å)	10.877(3)	13.408(4)
α (°)	99.677(9)	86.933(2)
β (°)	95.437(9)	84.680(3)
γ (°)	103.089(8)	81.508(3)
Volume ($Å^3$)	991.50(5)	1153.10(6)
Z	2	2
Density (gcm^{-3})	1.20	1.19
μ (mm^{-1})	0.077	0.075
F (000)	380.0	443.9
$h_{min, max}$	-11,11	-10,10

$k_{min, max}$	-13,13	-13,13
$l_{min, max}$	-13,13	-16,16
Reflections collected	21008	23543
Independent reflections	3862	4529
$R_{\_all}$, $R_{\_obs}$	0.1079, 0.053	0.109, 0.052
wR_{2_all}, wR_{2_obs}	0.1590, 0.1352	0.103, 0.042
$\Delta\rho_{min,max}$ (e Å^{-3})	-0.175, 0.136	-0.188, 0.207
GOOF	0.994	1.059

CRYSTAL STRUCTURE ANALYSIS FOR COMPOUND 4a

In general, it is difficult to grow superior quality crystals of mesogenic compounds carrying flexible alkoxy chains. In spite, we could obtain high-quality colorless block shaped crystals of compound **4a** by slow evaporation of solution (chloroform and methanol in 1:1 ratio). Its crystal structure was determined by SCXRD and the procured crystal data are presented in Table 2. The compound crystallizes in triclinic centrosymmetric space group *P-1* and cell parameters are *a*=8.978(3) Å, *b*=10.677(3) Å, *c*=10.877(3) Å, *V*=991.50(5) Å^3 with *Z*=2. Its molecular structure with atom labeling is shown in Figure 4. Interestingly, the structure was found to be non-planar as evidenced by the observed large torsion angle of 29.4(3)° (C9-C8-C5-C4) made by 4-cyanophenyl ring with the central pyridine ring and an angle of 8.1(3)° (C14-C13-C11-N1) made by 4-(butoxy)phenyl ring with the central pyridine ring. The butoxy chain is completely staggered and almost planar with respect to the benzene ring. As depicted in Figure 5, the structure involves in various kinds of intra- and inter-molecular interactions, viz. C-H…N, C-

H…π, C-H…O with the four neighboring molecules. Here, a C-H…N inter-molecular hydrogen bond (i.e., between nitrogen atom of terminal cyano group of one molecule and the nearby aromatic protons of another) and a C-H…N intra-molecular hydrogen bond (i.e., between the central pyridine ring and the neighboring aromatic protons of the molecule) were observed (Table 3). Further, C-H… π and C-H…O short contacts with the bond distance of 2.771 and 2.609 Å, respectively were noticed. Though, the molecule possesses slightly distorted structure, the observed values of bond lengths in the three ring system are restraining partial double bond character, suggesting the presence of delocalized π-electrons. Conclusively, the short contacts and molecular association observed in the crystal structure of **4a** contribute to the appearance of nematic phase in its LC state.

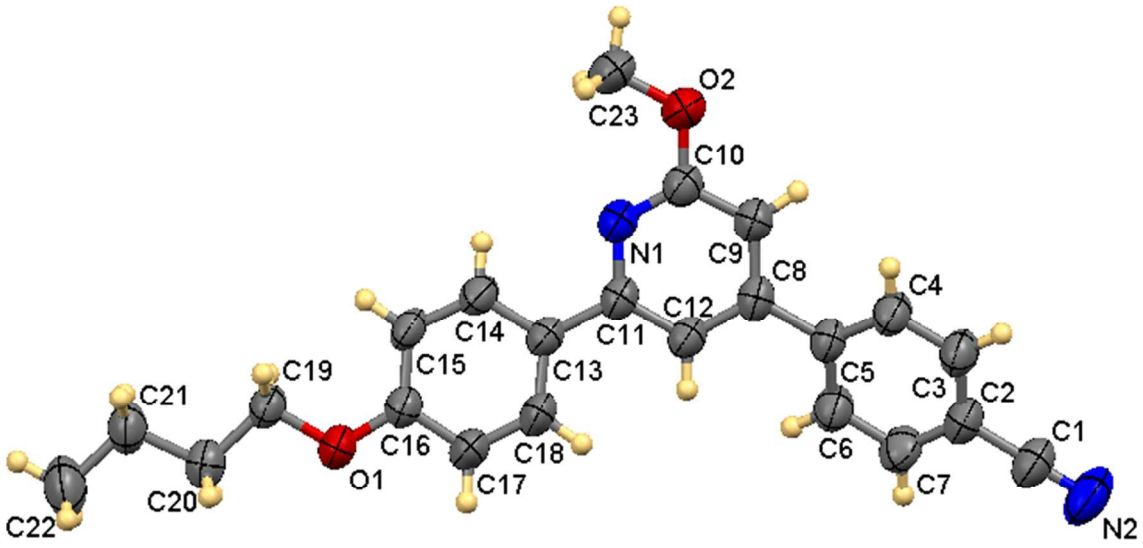

Figure 4. ORTEP diagram of 4-(2-(4-butoxyphenyl)-6-methoxypyridin-4-yl)benzonitrile (**4a**) with atom numbering.

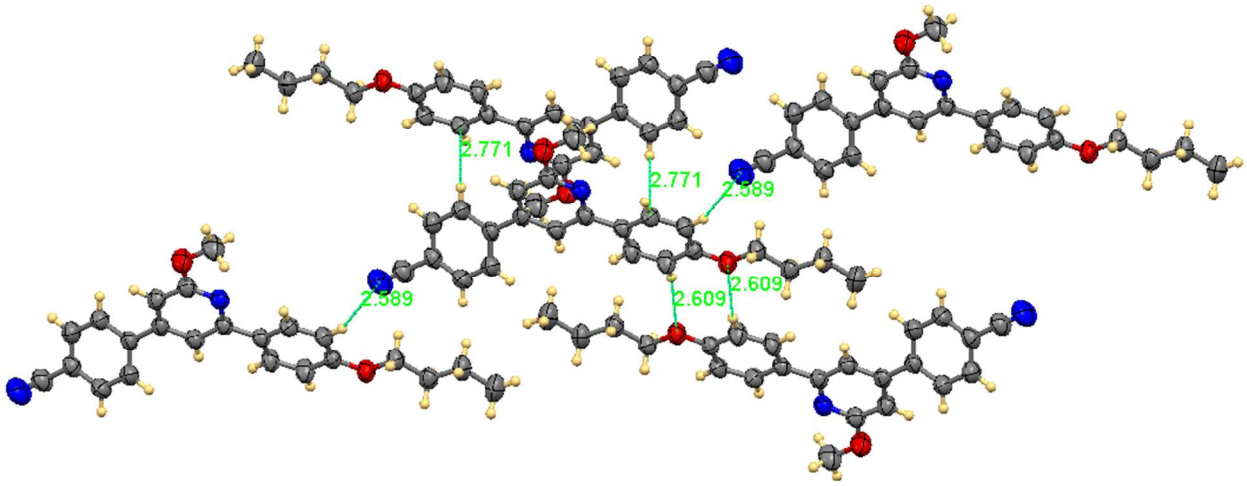

Figure 5. Packing diagram of compound **4a** showing various kinds of short contacts with their distances.

Table 3. Intra- and inter-molecular C-H…N interactions in the crystal structure of compound **4a**

Compound	D-H···A	D-H/Å	H···A/Å	D···A/Å	∠D-H···A/°	Symmetry
4a	C14-H14…N1	0.930	2.460	2.799(3)	101.00	x, y, z
	C15-H15...N2	0.930	2.590	3.460(3)	156.00	x+1,y-1,z

CRYSTAL STRUCTURE ANALYSIS FOR COMPOUND 4c

High-quality colorless block shaped crystals of compound **4c** were obtained by slow evaporation of solution (chloroform and methanol in 1:1 ratio). SCXRD experiment was carried out at 120 K and the obtained crystal data are presented in Table 2. Its ORTEP diagram with atom labeling is shown in Figure 6. The study revealed that crystal structure belongs to the triclinic centrosymmetric space group *P-1* and cell parameters are a=8.148(3) Å, b=10.726(3) Å, c=13.408(4) Å, V=1153.11(6) Å^3 with Z=2. In asymmetric unit the similar molecules are held together by C-H…N interactions (Figure 7). It is observed that the crystalline order formed by

intermolecular interactions is found to be similar to that of the columnar assembly, when the packing diagram is viewed along the *c* axis. Here, molecules are arranged one above the other in an anti-parallel manner.

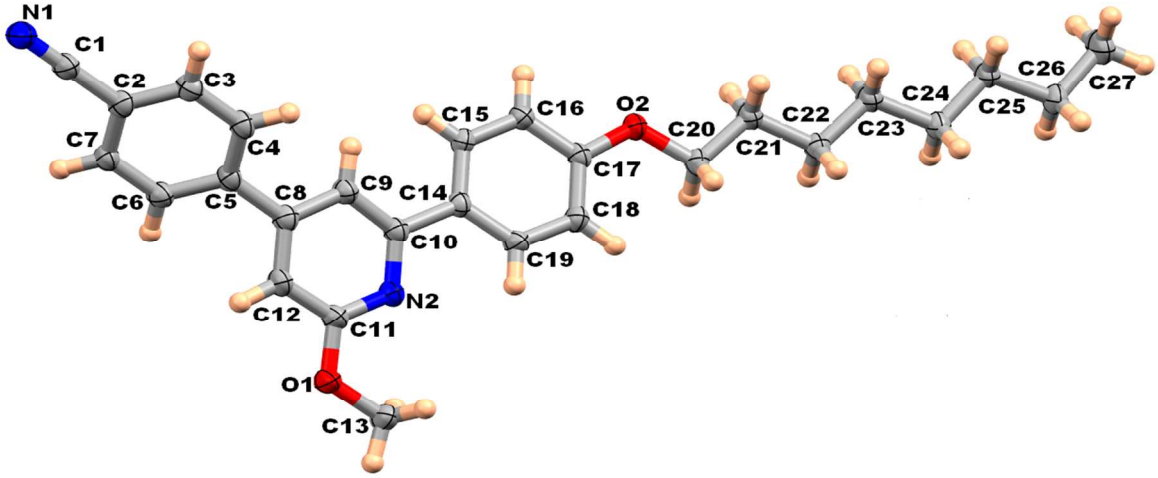

Figure 6. ORTEP diagram of 4-(2-methoxy-6-(4-(octyloxy) phenyl) pyridin-4-yl) benzonitrile (**4c**) with atom numbering.

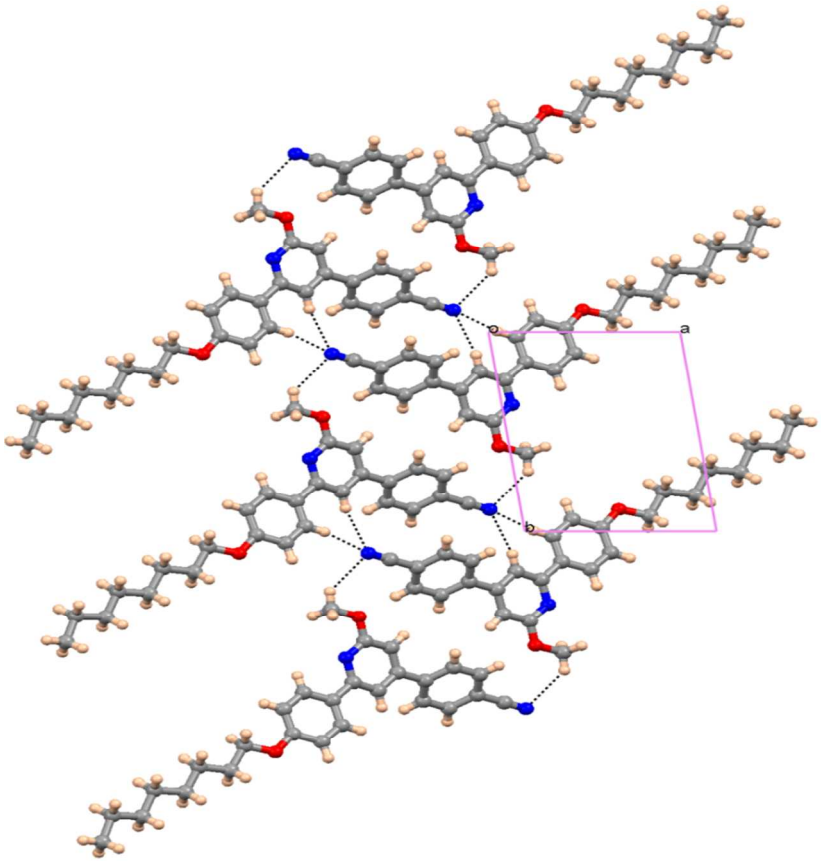

Figure 7. Packing diagram of compound **4c** depicting C-H…N intermolecular interactions and column-like structure.

From the crystallographic data, the compound **4c** is found to be non-planar and slightly more distorted than the molecular structure of **4a**, as evidenced by the observed large torsion angles of -39.9(2)° (C6-C5-C8-C12) made by the 4-cyanophenyl ring with the central pyridine ring and torsion angles of -15.1(2)° (N2-C10-C14-C19) made by the 4-(octyloxy)phenyl ring with the central pyridine ring. The observed torsion angles of 3.1(2)° (C13-O2-C11-N2) around the methoxy group substituted at position-6 of pyridine are slightly different. The octyloxy chain of molecule in the crystal system is also completely staggered and almost planar with respect to the benzene ring. Moreover, the terminal cyano group is in the same plane with respect to the benzene ring. In addition, its crystal structure exhibited several intra- and inter-molecular

interactions with the six neighboring molecules. These includes one kind of non-conventional C19-H19···N2 intra molecular H-bond formed by the central pyridine moiety and the neighboring aromatic proton of the molecule with the bond distance of 2.49 Å (Table 4). Also, two kinds of (i.e. C9-H9···N1 and C15-H15···N1) inter-molecular hydrogen bonds, formed by nitrogen atom of terminal cyano group of one molecule and the nearby aromatic protons of another, with the bond distance of 2.54 and 2.60 Å, respectively, are present. Its structure involves more number of short contacts (viz. C-H…π, and C-H…O) with the six neighboring molecules than the number of short contacts observed in case of **4a (**only four neighboring molecules). Thus, it can be concluded that the observed molecular arrangements and their association in solid state may be responsible for appearance of columnar phase in LC state of **4c**.

Table 4. Intra- and inter-molecular C-H…N interactions in the crystal structure of compound **4c**

Compound	D-H···A	D-H/Å	H···A/Å	D···A/Å	∠D-H···A/°	Symmetry
	C9-H9…N1	0.9500	2.5400	3.471(18)	165.00	-1-x,-y,1-z
4c	C15-H15...N1	0.9500	2.600	3.523(18)	163.00	-1-x,-y,1-z
	C19-H19…N2	0.9500	2.4900	2.821(17)	100.00	x, y, z

OPTICAL PROPERTIES

The UV-visible absorption and fluorescence emission spectra of compounds **4a-f** were recorded over the range of wavelength (λ), in chloroform solution at the concentration of 10^{-5} M and 10^{-6} M, respectively. The results are summarized in Table 5. The UV-visible absorption and

fluorescence emission spectra of compound **4a** are shown in Figure 8. In the absorption spectra of **4a-f**, a strong absorption band (λ_{abs}) was observed in the range of 335 to 345 nm and their spectra were found to be similar in shape because of their structural similarities. The fluorescence emission spectra of compound (**4a-f)** were recorded in chloroform solution at λ_{exc}=330 nm. Interestingly, all of them were found to be luminescent and showed a broad blue light emission band (λ_{em}) in the visible region (415-425 nm). This observed blue light emission may be attributed to extended conjugation of cyano group in association with the mesogenic core.[31] Further, their fluorescence quantum yields ($\mathbf{\Phi_f}$) in solution state were determined using the method described by Demas and Crosby, with quinine sulphate in degassed 0.1M sulphuric acid as reference standard (Φ_f = 54 %).[32] Accordingly, the compounds exhibited good quantum yield in the range of 42-50 % in their solution state. Further, the fluorescence spectra were recorded for the thin films of compounds **4a-f** in their solid phase. The requisite thin films of solid phase were obtained over the glass slide by spin coating the solution of compounds in chloroform. The prepared thin films exhibited strong blue fluorescence emission band in the range of 434-460 nm in solid phase with quite considerable absolute quantum yields of Φ_f = 5-13%.[33] In fact, their emission band was significantly broadened and red shifted (~20-40 nm) in solid phase compared to the emission band in solution state.

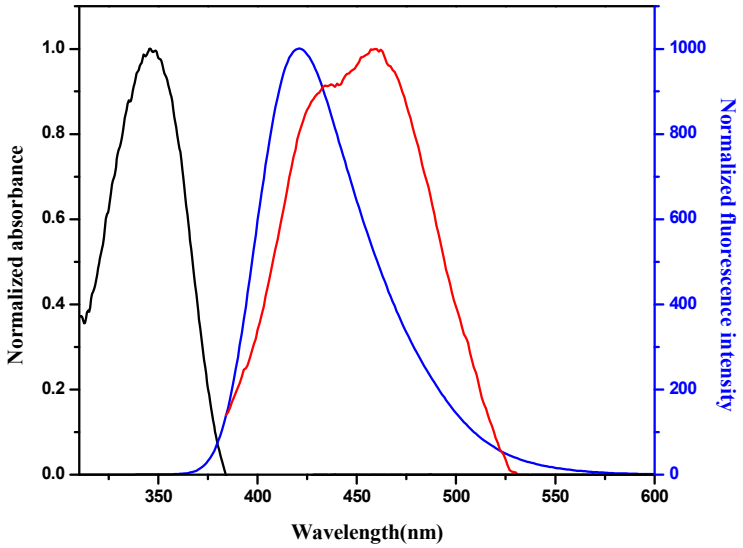

Figure 8. UV-visible (black line) and fluorescence spectra (blue line) of **4a** in chloroform solution and solid phase (red line) at room temperature.

Table 5. UV-visible absorption and fluorescence emission properties of **4a-f**

Compound	λ_{abs} /nm	λ_{em} (solution) / nm	Φ_f (solution)/%	λ_{em} (solid phase) / nm	Φ_f (solid phase)/%
4a	345	421	43	460	5.01
4b	340	416	50	448	7.40
4c	340	418	48	452	5.60
4d	339	418	49	444	6.82
4e	336	418	42	453	5.88
4f	336	417	45	434	12.15

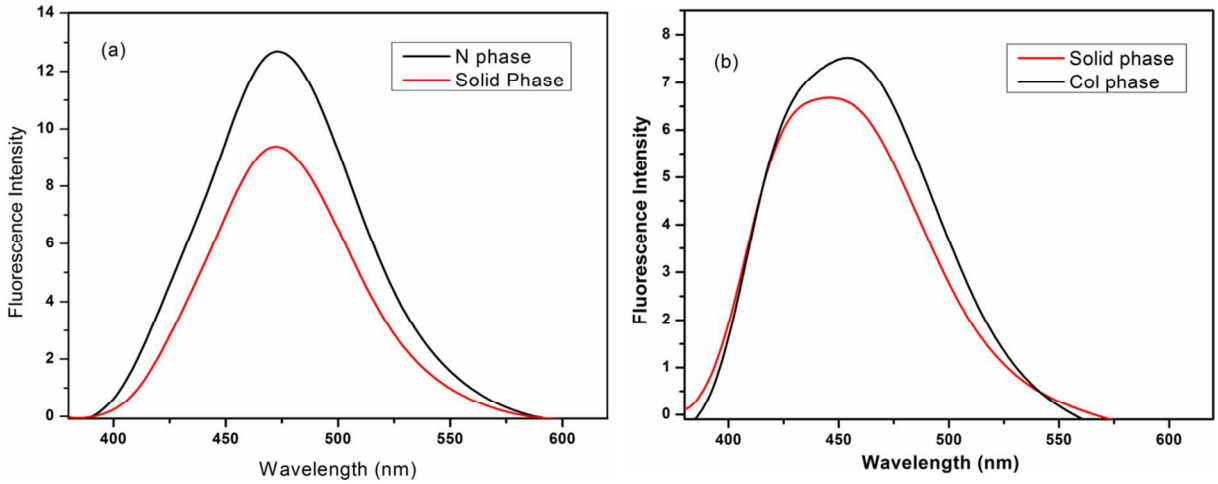

Figure 9. Fluorescence spectra in solid and LC phase for (a) **4a** (b) **4f**

In order to determine the emission behavior in LC phase, representative compounds **4a** and **4f** were selected. In the experiment, thin film of the sample was prepared by keeping the compound in between the two coverslips and it was cooled slowly to obtain the LC phase from isotropic state. The florescence spectra were recorded in their LC state and the obtained emission patterns were compared with the spectra of their solid phase (Figure 9). As per the results, the compounds **4a** and **4f** display blue emission with maximum intensity as well as slight broadening in the curve area compared to their emission in solid phase. The emission spectrum of **4a** in nematic phase (at 135 °C) shows no shift in the emission band. However, the increased intensity in the emission band was noticed when compared to that of solid phase. Similarly, emission spectrum of **4f** in orthorhombic columnar phase (at 105 °C) exhibits the increase in emission intensity. In addition, a slight red shift (10 nm) was observed in the emission band compared to its emission behavior in solid phase.[34,35] These observations are mainly attributed to the favorable molecular arrangements in LC phase of **4a** and **4f**. Conclusively, the target compounds **4a-f** have emerged

as promising blue fluorescent materials and can be used as emissive dopants in an electroluminescent device.

ELECTROCHEMICAL PROPERTIES

Electrochemical behavior of **4c** was investigated by cyclic voltammetry (CV) in order to determine its redox behavior as well as HOMO and LUMO energy levels. CV measurement was carried out at 25 °C in dry acetonitrile solution containing 0.1 M Bu_4NPCl_4 as supporting electrolyte, glassy carbon as working electrode, Pt wire as counter electrode and Ag/AgCl as reference electrode with a scan rate of 50 mV/s.[36] Also, the instrument was calibrated using ferrocene as internal standard[37] The cyclic voltammogram of **4c** is shown in Figure 10. It represents two single electron onset oxidation potentials at +0.66 and +1.54 V during anodic cycle as well as one onset reduction potential at -1.23V during cathodic cycle. The first onset oxidation potential and reduction potential values were used for the calculation of HOMO and LUMO energy levels by using equations, $E_{HOMO} = -[E_{onset}^{oxd} + 4.4eV]$ and $E_{LUMO} = -[E_{onset}^{red} + 4.4eV]$, where E_{onset}^{oxd} and E_{onset}^{red} are the observed onset oxidation and onset reduction potentials verses standard calomel electrode. It's HOMO and LUMO energy levels were found to be -5.06 and -3.17 eV, respectively. Thus, the electrochemical band gap was calculated to be 1.89 eV. Similarly, the rest of compounds of the series are expected to show the identical behavior in the CV experiments, because of their structural similarities and the negligible influence of variable terminal alkoxy chains on their electronic properties.

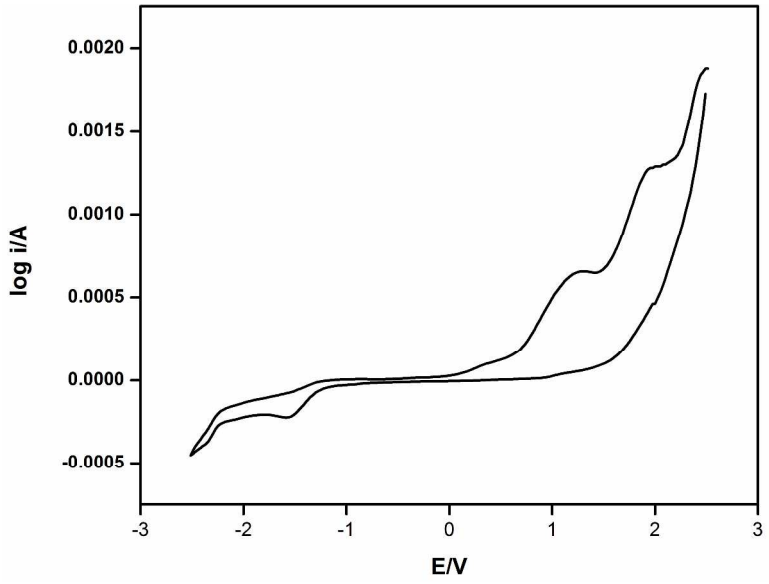

Figure 10. Cyclic voltammogram of **4c**.

THEORETICAL CALCULATION

A complete geometrical optimization on compound **4c** was implemented within the C_1 point group symmetry at RI-DFT method with def2-TZVP [38,39] basis sets by using Turbomole [40] software package. Figure 11 shows the optimized molecular geometry and it possesses a nonplanar structure. Also, the geometry is same as that of the molecular conformation observed in its crystal structure. Further, HOMO and LUMO energy levels of **4c** were calculated and its frontier molecular orbitals (FMO) are shown in Figure 12. This illustrates that π orbitals of HOMOs are localized on the 2-(4-(hexyloxy)phenyl)-6-methoxypyridine moiety and π* orbitals of LUMOs are delocalized on the electron-accepting 4-(6-methoxypyridin-4-yl)benzonitrile segment. Thus, the observed FMO indicates that the molecule has good intra-molecular charge transfer ability. Further, to get theoretical absorption spectrum, DFT method was performed on nonplanar compound **4c** by using def-TZVP basis sets. Its theoretical spectrum showed a strong absorption band at 341 nm (Figure 13) and is in accordance with that of the experimentally

obtained absorption band of 340 nm. This strong absorption band is due to the energetically more favorable π→π* transitions arising from the highest energy bonding pi-orbital (HOMO) to the lowest energy anti-bonding pi-orbital (LUMO).

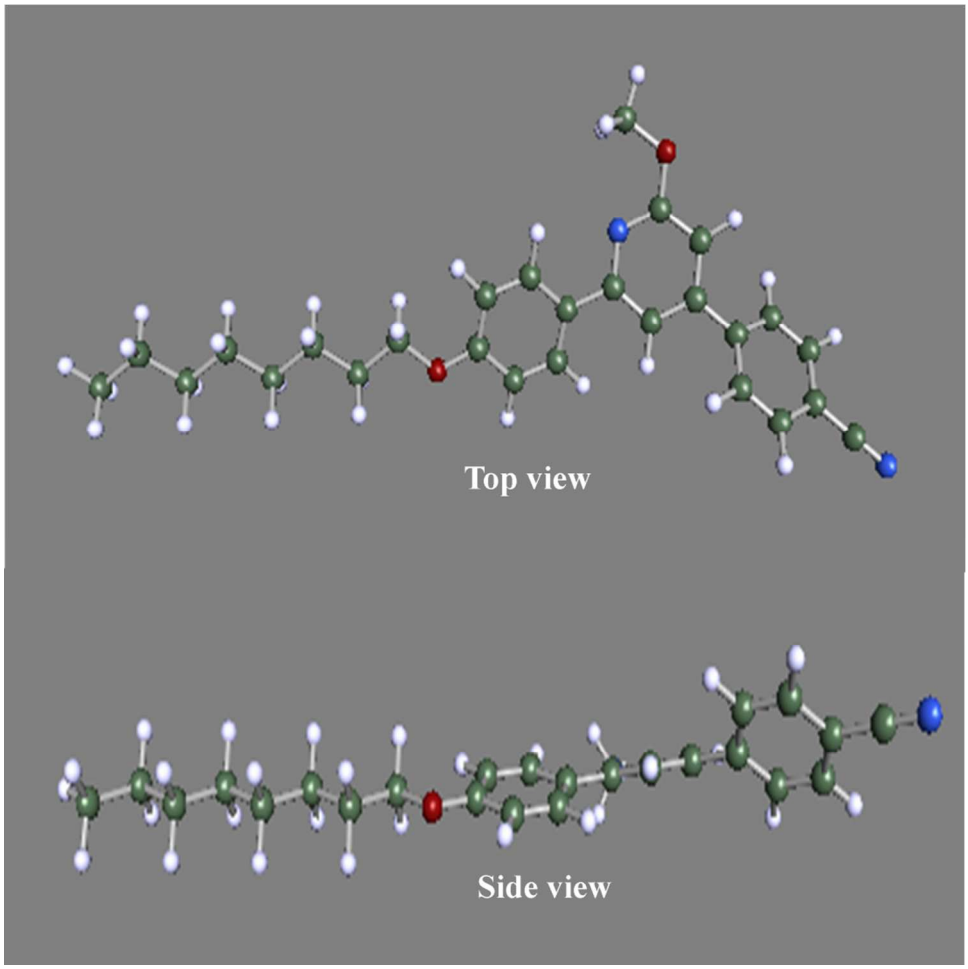

Figure 11. Optimized geometry of **4c**.

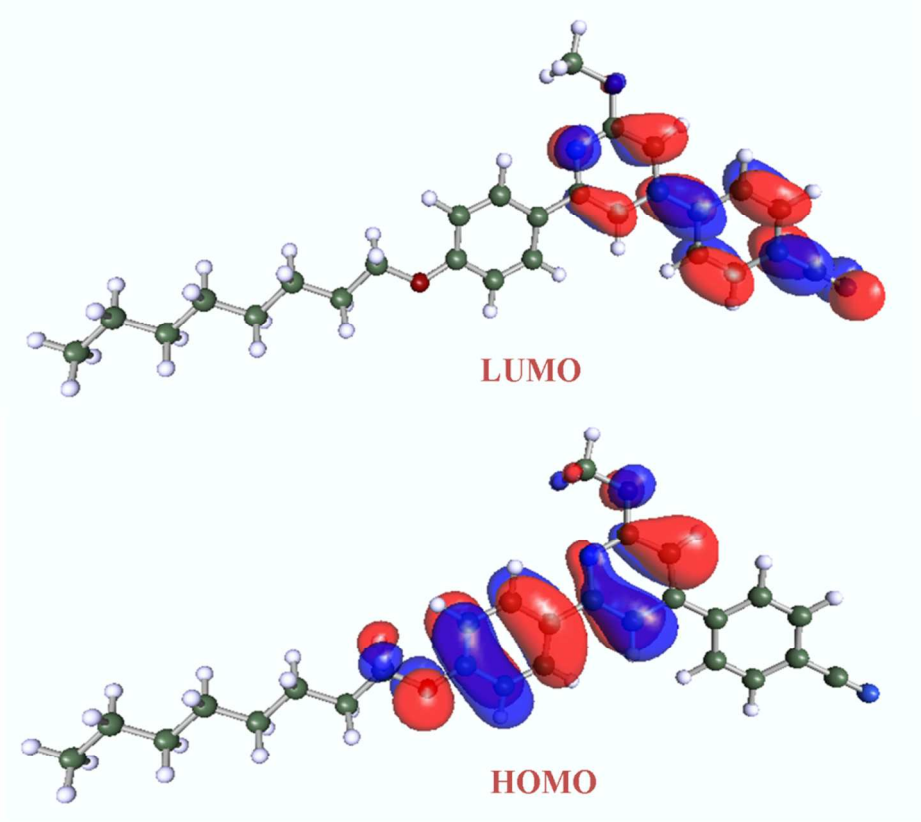

Figure 12. Frontier molecular orbitals of **4c**.

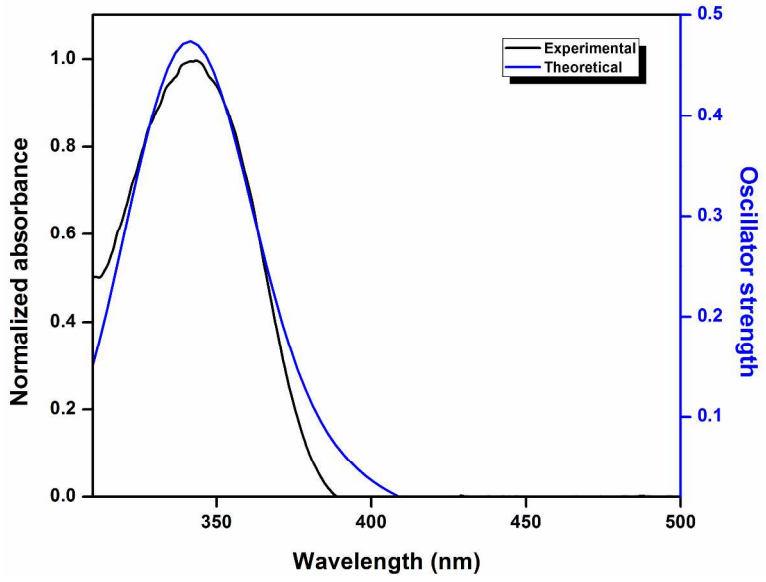

Figure 13. Experimental (black line) and theoretical (blue line) calculated absorption electronic spectra of **4c**.

CONCLUSION

In summary, a new series comprising six luminescent, and bent shaped liquid crystalline compounds (**4a-f**) based on methoxypyridine as central core was synthesized successfully and characterized by spectral methods. Their POM, DSC and PXRD studies reveal that compound **4a** exhibit nematic phase, while the remaining compounds exhibit orthorhombic columnar phase. The single crystal X-ray analysis supports that the molecules possess bent shaped structure with slightly non-planar confomations and existence of short contacts. Further, the DFT calculations support the distorted structure. The optical studies reveal that the compounds are blue emissive materials with good quantum yield. The compounds were found to possess low electrochemical band gap of 1.89 eV with good charge transport ability.

† Electronic supplementary information (ESI) available: Materials and methods, synthetic procedures, single crystal X-ray crystallography studies, powder X-ray diffraction studies and optical properties. Crystallographic data for the structure reported in this article have been deposited with the Cambridge Crystallographic Data Center with the deposition numbers 909202 and 958625. Copy of the data can be obtained free of charge from the Director, CCDC, 12 Union Road, Cambridge CB2 1EZ, UK [Fax: +44-1223-336-033; E-mail: deposit@ccdc.cam. ac.uk or www.ccdc.cam.ac.uk].

ACKNOWLEDGMENTS

The authors are grateful to the NITK, Surathkal, NMR research centre, Solid State Structural Chemistry Unit, IISc, Centre for Soft Matter Research, and Soft Condensed Matter Group, RRI, Bangalore, India for necessary facilities.

REFERENCES

1. D. Bauman, A. Skibinski, R. Stolarski, *Mol. Cryst. Liq. Cryst.*, 1986, **138**, 367.
2. T. Martyński, E. Mykowska, D. Bauman, *J. Mol. Struct.*, 1994, **325**, 161.
3. H. J. Coles, G. A. Lester, H. Owen, *Liq. Cryst*., 1993, **14**, 1039.
4. A. Beer, G. Scherowsky, H. Owen, H. Coles, *Liq. Cryst.*, 1995, **19**, 565.
5. E. Thikonov, M. Bertolotti, F. Scudieri, *Appl. Phys.*, 1976, **11**, 357.
6. M. Bertolotti, G. Sansoni, F. Scudieri, *Appl. Opt.*, 1979, **18**, 528.
7. S. Kuroda, K. Kubota, *Appl. Phys. Lett.*, 1976, **29**, 737.
8. T. Christ, B. Glusen, A. Greiner, A. Kettner, R. Sander, V. Stumpflen, V. Tsukruk, J. H. Wendorff, *Adv. Mater.*, 1997, **9**, 48.
9. T. Christ, V. Stümpflen, J. H. Wendorff, *Macromol. rapid Commun.*, 1997, **18**, 93.
10. S. Benning, H.-S. Kitzerow, H. Bock, M.-F. Achard, *Liq. Cryst.*, 2000, **27**, 901.
11. J. Simmerer, B. Glüsen, W. Paulus, A. Kettner, P. Schuhmacher, D. Adam, K.-H. Etzbach, K. Siemensmeyer, J. H. Wendorff, H. Ringsdorf, and D. Haarer, *Adv. Mater*., 1996, **8**, 815.
12. H. Gallardo, G. Conte, P. A. Tuzimoto, B. Behramand, F. Molin, J. Eccher, I. H. Bechtold, *Liq. Cryst.*, 2012, **39**, 1099.
13. E. Beltrán, J. L. Serrano, T. Sierra, R. Giménez, *Org. Lett.*, 2010, **12**, 1404.
14. Y. Sagara, T. Kato, *Angew. Chem., Int. Ed.*, 2011, **50**, 9128.

15. M. P. Aldred, R. Hudson, S. P. Kitney, P. Vlachos, A. Liedtke, K. L. Woon, M. O'Neill, S. M. Kelly, *Liq. Cryst.*, 2008, **35**, 413.

16. A. K. Prajapati, V. Modi, *Liq. Cryst.*, 2010, **37**, 407.

17. P. A. Paraskos, T. M. Swager, *Chem. Mater.*, 2002, **14**, 4543.

18. Y.-T. Shen, C.-H. Li, K.-C. Chang, S.-Y. Chin, H.-A. Lin, Y.-M. Liu, C.-Y. Hung, H.-F. Hsu, S.-S. Sun, *Langmuir*, 2009, **25**, 8714.

19. S. Moyano, J. Barberá, B. E. Diosdado, J. L. Serrano, A. Elduque, R. Giménez, *J. Mater. Chem. C*, 2013, **1**, 3119.

20. D. D. Prabhu, N. S. S. Kumar, A. P. Sivadas, S. Varghese, S. Das, *J. Phys. Chem. B*, 2012, **116**, 13071.

21. R. Cristiano, D. M. P. de Oliveira Santos, G. Conte, H. Gallardo, *Liq. Cryst.*, 2006, **33**, 997.

22. T. N. Ahipa, V. Kumar, A. V. Adhikari, *Struct. Chem.*, 2014, 1.

23. K. A. Vishnumurthy, M. S. Sunitha, K. Safakath, R. Philip, A. V. Adhikari, *Polymer*, 2011, **52**, 4174.

24. V. N. Kozhevnikov, S. J. Cowling, P. B. Karadakov, and D. W. Bruce, *J. Mater. Chem*., 2008, **18**, 1703.

25. F. E. Goda, A. A. M. Abdel-Aziz, O. A. Attef, *Bioorg. Med. Chem.*, 2004, **12**, 1845.

26. M. M. Al-Arab, H. D. Tabba, L. A. Abu-Yousef, M. O. Marilyn, *Tetrahedron*, 1988, **44**, 7293.

27. M. M. Al-Arab, *J. Heterocycl. Chem.*, 1989, **26**, 1665.

28. C. Keith, A. Lehmann, U. Baumeister, M. Prehm, and C. Tschierske, *Soft Matter*, 2010, **6**, 1704.

29. M. Lehmann, M. Jahr, B. Donnio, R. Graf, S. Gemming, and I. Popov, *Chemistry – A European Journal*, 2008, **14**, 3562.

30. M. Peterca, M. R. Imam, C.-H. Ahn, V. S. K. Balagurusamy, D. A. Wilson, B. M. Rosen, and V. Percec, *J. Am. Chem. Soc.*, 2011, **133**, 2311.

31. J. Han, M. Zhang, F. Wang, Q. Geng, *Liq. Cryst.,* 2010, **37**, 1471.

32. J. N. Demas, G. A. Crosby, *J. Phys. Chem.,* 1971, **75**, 991.

33. Y. Kawamura, H. Sasabe, C. Adachi, *Jpn. J. Appl. Phys., Part 1,* 2004, **43**, 7729.

34. F. Würthner, C. Thalacker, S. Diele, and C. Tschierske, *Chemistry – A European Journal*, 2001, **7**, 2245.

35. J. Seo, S. Kim, S. H. Gihm, C. R. Park, and S. Y. Park, *J. Mater. Chem.*, 2007, **17**, 5052.

36. J. Heinze, *Angew. Chem*., 1984, **96**, 823.

37. J. Pommerehe, H. Vestweber, W. Guss, R. F. Mahrt, H. Bassler, M. Porsch, J. Daub, *Adv. Mater.*, 1995, **7**, 55.

38. F. Weigend, *Phys. Chem. Chem. Phys.*, 2006, **8**, 1057.

39. F. Weigend, R. Ahlrichs, *Phys. Chem. Chem. Phys*., 2005, **7**, 3297.

40. R. Ahlrichs, M. Bär, M. Häser, H. Horn, C. Kölmel, *Chem. Phys. Letters,* 1989, **162**, 165.

Graphical abstract: